NASA Contractor Report 185254

Feasibility Study for the Advanced One-Dimensional High Temperature Optical Strain Measurement System—Phase III

Christian T. Lant
Sverdrup Technology, Inc.
Lewis Research Center Group
Brook Park, Ohio

June 1990

Prepared for
Lewis Research Center
Under Contract NAS3-25266

National Aeronautics and
Space Administration

FEASIBILITY STUDY

FOR THE ADVANCED ONE-DIMENSIONAL

HIGH TEMPERATURE

OPTICAL STRAIN MEASUREMENT SYSTEM

– Phase III

Christian T. Lant
Sverdrup Technology, Inc.
NASA Lewis Research Center Group
Brook Park, Ohio 44142

SUMMARY

The Instrumentation and Control Technology Division is developing optical strain measurement systems for applications using high temperature wire and fiber specimens. This feasibility study has determined that stable optical signals can be obtained from specimens at temperatures beyond 2,400°C. A system using an area array sensor is proposed to alleviate off-axis decorrelation arising from rigid body motions. A digital signal processor (DSP) is recommended to perform speckle correlations at a rate near the data acquisition rate. Design parameters are discussed, and fundamental limits on the speckle shift strain measurement technique are defined.

INTRODUCTION

The primary purpose of this study is to determine the feasibility of making one-dimensional strain measurements on a hot wire specimen, using the speckle-shift strain measurement technique.[1] The Phase I effort produced a strain measurement system based on the one-dimensional speckle-shift technique of Yamaguchi. This system explored limits on the technique and measured strains on a flat specimen at 450° Celsius. Phase II expanded the system's capabilities by providing two-dimensional strain measurements, reducing error, and increasing throughput. Two-dimensional strains were measured at 650°C, with stable speckle patterns recorded above 750°C.

The development of advanced materials suitable for use in very high temperature engine applications extends the requirements on instrumentation used to characterize these materials and verify models of component parts. In particular, accurate static strain measurements on specimens in the temperature regime of 1000° to 2000°C are needed. Strain measurements in this regime have rarely been demonstrated. Optra Inc.'s laser extensometer technique has been used to measure strain to 1100°C,[2] and resistance strain gages have made static measurements at 700° to 800°C, but with large apparent strains.[3-5] Since optical measurements are often degraded by refractive index variations at high temperatures,[6] the question remains whether the speckle-shift strain measurement technique is inherently susceptible to adverse thermal effects in this temperature regime.[7-8]

This study answers fundamental questions which will aid the development of an advanced speckle-shift strain measurement system (Phase IV):

- Are the speckle-shift relations valid for small diameter wire specimens?
- Can accurate correlations be performed at temperatures ranging from 1000° to 2000°C?
- What are the requirements for real time 1-D measurement systems?

The results of this study are obtained both analytically and experimentally. A number of system design parameters are discussed in detail.

SPECKLE–SHIFT TECHNIQUE

A brief description of the speckle-shift technique is given here (see the references for more detail). Two symmetrically incident laser beams, beam 1 and beam 2, are reflected sequentially off a point on a test specimen. The resulting speckle patterns are recorded by a sensor array camera. After straining the specimen, another pair of speckle patterns are recorded. These after-strain patterns have now been shifted slightly, relative to the original "reference" patterns, parallel to the surface of the specimen along the plane of incidence of the laser beams. A cross-correlation of the reference and shifted patterns gives the distance each pattern shifted, which is directly proportional to the strain on the specimen parallel to the plane of incidence. The use of two symmetrical beams allows terms of speckle pattern shift due to rigid body motions of the specimen to be cancelled automatically.

Consider a geometry, shown in Figure 1, such that an electronic sensor array is located in the X,Y plane, and the source (specimen surface) is defined to be in the x,y plane. The x,y and X,Y planes are separated by a distance L_0 along the z axis. Two-dimensional deformation of object points on the specimen are described by vector **a**(x,y), and the resulting shifts of the speckle pattern are given by vector A(X,Y). The shaded rectangle in the figure indicates a one-dimensional reference slice of the speckle pattern, shifted from the origin by A(X,Y). The x,z plane is the plane of the incident laser beam, which makes the x axis the sensitive axis. The simplified speckle-shift relations for the X and Y components are given by:

$$A_X = a_x - L_0\left[\epsilon_{xx}\cdot\sin(\theta_S) - \Omega_y\left[\cos(\theta_S) + 1\right]\right] \qquad (1.a)$$

$$A_Y = a_y - L_0\left[\epsilon_{xy}\cdot\sin(\theta_S) + \Omega_x\left[\cos(\theta_S) + 1\right] - \Omega_z\cdot\sin(\theta_S)\right] \qquad (1.b)$$

where θ_S is the incident angle of the laser beam, and Ω is the rotation vector with components

$$(\Omega_x\ ,\ \Omega_y\ ,\ \Omega_z) = \left[\left[\frac{\partial a_z}{\partial y}\right]_0\ ,\ -\left[\frac{\partial a_z}{\partial x}\right]_0\ ,\ \frac{1}{2}\left[\left[\frac{\partial a_y}{\partial x}\right]_0 - \left[\frac{\partial a_x}{\partial y}\right]_0\right]\right] \qquad (2)$$

The terms ϵ_{xx} and ϵ_{xy} are two components in the strain tensor, given by:

$$\epsilon_{xx} = \left[\frac{\partial a_x}{\partial x}\right]_0 \qquad (3.a)$$

$$\epsilon_{xy} = \frac{1}{2}\left[\left[\frac{\partial a_y}{\partial x}\right]_0 + \left[\frac{\partial a_x}{\partial y}\right]_0\right] \qquad (3.b)$$

The strain component of interest is ϵ_{xx}. This component is extracted from Equation (1.a) by taking the difference between shifts $A_X(\theta_S{=}30^\circ)$ and $A_X(\theta_S{=}{-}30^\circ)$, representing beam 1 and beam 2, respectively. The strain is given in terms of this difference in shifts:

$$\epsilon_{xx} = \frac{-\Delta A_X}{2L_0\cdot\sin(\theta)} \qquad (4)$$

where $\theta{=}|\theta_S|$. Note that the principal strains only induce shift along the X axis. Under ideal conditions, off-axis shifts A_Y are negligible.

The values of A_X are determined by cross–correlating the reference and shifted speckle patterns f(x) and g(x), for each beam, according to the equation

$$R(\Delta x) = \frac{1}{2\chi}\int_{-\chi}^{\chi} f(x)\cdot g(x+\Delta x)\,dx \qquad (5)$$

The value of Δx for which the correlation function $R(\Delta x)$ has the greatest maximum is the distance the pattern shifted. Therefore, $A_X = \Delta x$.

This gives a 1-D component of strain along the intersection of the incident plane and the specimen surface. This technique has also been shown to make accurate two-dimensional strain measurements. To obtain a 2-D strain measurement at the gage point it is necessary to take a minimum of three one-dimensional strain measurements at different azimuthal angles on the specimen surface. From these three components one can calculate the 1st and 2nd principal strains and their orientation on the specimen.[8]

OPTICAL PARAMETERS

Previous applications of this technique have been on flat or slowly curving specimen shapes. The change in the specimen size and shape can be significant in the application. The transfer of the speckle-shift technique from flat specimens to wire specimens cannot be assumed trivial a priori, due to the large change in scale of the specimen parameters, and must be analyzed carefully.

The following sub-sections discuss in detail some important aspects of the optical system to consider when designing a speckle-shift strain measurement system for use with wire or fiber specimens.

Speckle Statistics and Detector Resolution

The pixel-to-speckle ratio (# of pixels per speckle = mean speckle diameter / pixel pitch) affects the accuracy of the cross-correlation. It is necessary to sample the fine structure of the speckle pattern to below the resolution of the smallest speckle in order to make the most use of the correlation technique. It is also prudent not to greatly oversample the speckle pattern, because the overall number of samples that can be taken is limited by the elements in the detector.

By using an optimum sampling interval the sampled frame includes the most information possible about the intensity distribution of the speckle pattern. Having more than the optimum number of pixels / speckle does not increase the information content, or spatial frequency bandwidth, of the image. Rather, it decreases the information about the speckle distribution by limiting the number of speckles that will fit on the array. The advantage of maximizing the information content is that if more information is read, the speckle pattern will look more unique in the correlation. This uniqueness of the speckle pattern reduces the chance of ambiguous correlations.

The minimum speckle size is inversely related to the effective aperture of the optical system. However, although the speckles change shape when using wire specimens with diameters smaller than the laser spot, the pixel-to-speckle ratio along the sensitive axis of the instrument remains unaffected. The discussion begins by describing the case where the spot falls completely on the specimen, and continues by adding the effect of a specimen narrower than the laser beam.

The parameter d, the spot diameter along the wire axis, is defined by the beam radius ω and incident angle θ_S:

$$d = \frac{2\omega}{\cos\theta_S} \tag{6}$$

As shown in Figure 2, the spot on the specimen becomes elliptical for a circular beam of non-normal incidence. The angle θ_S along the wire axis is 30° in the current setup.

When dealing with an elliptical spot there exists joint normality between the uncorrelated random variables x and y,[9] where the marginal densities of x and y are given by the Gaussian probability densities:

$$I_x(x) = I_0 \cdot e^{-\frac{1}{2}\left[\frac{x}{\sigma_x}\right]^2} \tag{7.a}$$

and

$$I_y(y) = I_0 \cdot e^{-\frac{1}{2}\left[\frac{y}{\sigma_y}\right]^2} \tag{7.b}$$

These intensities are the squares of the

electric fields. The laser spot diameters are related to the standard deviations σ_x and σ_y by the relationships

$$d \equiv 4 \cdot \sigma_x \qquad (8.a)$$

and

$$2\omega \equiv 4 \cdot \sigma_y \qquad (8.b)$$

The diffraction limited speckle radius r_X along the incident plane (parallel to the wire axis in this case) can be calculated using the Fraunhofer approximation to the standard diffraction integral. The aperture function in the integral is a 1-D Gaussian. The electric field of the "smallest speckle" in the sensor plane is given by:

$$E(x) = A \int_{-\infty}^{\infty} e^{\frac{-x^2}{4\sigma_x^2}} \cdot e^{\frac{-ik}{2L_0}(x^2 - 2xx)} \, dx \qquad (9)$$

where the propagation vector $k \equiv 2\pi/\lambda$, λ is the laser wavelength, and L_0 is the specimen-to-sensor distance. The phase shift introduced by the non-zero incident angle is dropped. Solving Equation (9) gives

$$E(x) = B\, e^{-\left[\frac{\sigma_x k x}{L_0}\right]^2} \qquad (10)$$

The intensity is the square of the electric field, so

$$I(x) = C\, e^{-2\left[\frac{\sigma_x k x}{L_0}\right]^2}$$

$$= C\, e^{\frac{-x^2}{2\sigma_X^2}} \qquad (11)$$

after defining

$$\sigma_X \equiv \frac{L_0}{2\sigma_x \cdot k} \qquad (12)$$

to be the standard deviation of the Gaussian in the sensor plane.

The measure of a Gaussian function's radius is typically taken to be two standard deviations from the Gaussian's mean position when defined as in Equation (11). The radius r_X is thus defined to be at the e^{-2} point of Equation (11), noting that

$$r_X = 2 \cdot \sigma_X \Rightarrow \frac{r_X^2}{2\sigma_X^2} = 2 \qquad (13)$$

Substituting Equation (12) into Equation (13) gives the radius of the intensity distribution of the "smallest" speckle:

$$r_X = \frac{L_0}{\sigma_x \cdot k} \qquad (14)$$

The diameters of the wires tested range from 76 to 813 μm (3 to 32 mils), which go from much smaller to slightly larger than the laser spot size (diameter) 2ω of 600 μm. For wires smaller than the spot size, the asymmetry of the diffraction limited optical system increases, and there occurs progressively greater elongation of the individual speckles in the Y direction of the sensor plane. The speckles take on an asymmetric two-dimensional intensity distribution: the width in the direction of the sensitive axis of the instrument is inversely proportional to the laser beam spot size on the wire, as is evident in Equation (14). Since σ_x is inversely proportional to $\cos\theta_S$, the width is also proportional to the cosine of the incident angle θ_S of the beam, as in the case of an extended flat specimen.

The transverse speckle width, on the other hand, changes with the specimen diameter due to truncation of the laser beam. This truncation is described as the product of a square aperture function (the reflection profile) with a Gaussian function. In the Fourier transform plane, the transform of the Gaussian is convolved with the transform of the square wave, broadening the speckle size accordingly. Denoting the Gaussian function by $f_1(y)$ and the square aperture function by $f_2(y)$ we can describe the speckle profile in the Y direction as $F_s(Y)$:

$$F_s(Y) = F_s(\kappa_Y) \quad \text{where } Y \propto \kappa\Big|_{z=L_0}$$

$$= \mathcal{F}\Big\{f_1(y)\cdot f_2(y)\Big\}$$

$$= \mathcal{F}\Big\{f_1(y)\Big\} * \mathcal{F}\Big\{f_2(y)\Big\} \qquad (15)$$

In Equation (15) $\mathcal{F}$ is the Fourier transform operator and $*$ is the convolution operator. The variance of the convolution of two functions is equal to the sum of the variances.[10] If the widths of the two functions are taken by the root-mean-square (rms) deviations σ_1 and σ_2 of their transforms F_1 and F_2, then the width of the speckles in the Y direction σ_Y is given by:

$$\sigma_Y = \sqrt{\sigma_1^2 + \sigma_2^2} \qquad (16)$$

The speckle width in the transverse direction Y is related to the widths of the Fourier transforms of the wire reflection profile and the Gaussian beam. Equation (16) thus takes into account that the Gaussian distribution of the beam is truncated by the edges of the wire.

It is clear that the wire diameter has no effect on the pixel-to-speckle ratio along the axis of interest. Using Equation (14) to calculate the speckle size, the pixel-to-speckle ratio for the Phase II system, with a pixel pitch of 15 μm, L_0=1 m, 2ω=600 μm, θ_S=30°, and λ=514.5 nm, was 63 pixels/speckle diameter.

It also follows that the validity of the generic speckle-shift relations holds true for longitudinal strains on a small diameter specimen. The longitudinal speckle statistics do not change from those in the case of a flat specimen.

At first it may seem that the conclusions of the preceding analysis obviate the usefulness of the analysis itself. However, two-dimensional shifts do occur during tests, and knowledge of the transverse speckle widths gives a measure of the decorrelation distance when using a linear sensor array. In addition, the results are useful for two-dimensional strain measurements, where shifts along the transverse axis must be measured.

The optimum sampling frequency in the X direction is estimated to be the Nyquist sampling frequency, which is twice the highest spatial frequency present in any slice of the speckle pattern in the X direction. The spectral power density of the Gaussian is found by taking the Fourier transform of the exponential in Equation (11):

$$\mathcal{F}\left\{e^{\frac{-x^2}{2\sigma_X^2}}\right\} = \sqrt{2\pi}\,\sigma_X\cdot e^{\frac{-1}{2}(\sigma_X\kappa)^2} \qquad (17)$$

The cut-off spatial frequency κ_c is again chosen to be the e^{-2} point, now of the Gaussian spectral power density. By equating the exponent in the right of Equation (17) to –2 and solving for κ_c

$$\kappa_c = \frac{2}{\sigma_X}$$

$$= \frac{4\sigma_x\cdot k}{L_0} \qquad (18)$$

The Nyquist frequency

$$\kappa_N = 2\cdot\kappa_c \qquad (19)$$

then is proportional to the inverse of the optimum sampling interval a_N:

$$a_N = \frac{2\pi}{\kappa_N}$$

$$= \frac{\pi L_0}{4\sigma_x\cdot k} \qquad (20)$$

This gives a pixel-to-speckle ratio of

$$\frac{2 \cdot r_X}{a_N} = \frac{2 \cdot \left[\frac{L_0}{\sigma_x \cdot k}\right]}{\frac{\pi L_0}{4\sigma_x \cdot k}}$$

$$= \frac{8}{\pi} = 2.55 \left[\frac{\text{pixels}}{\text{speckle}}\right] \qquad (21)$$

To conclude, Equation (21) suggests that a sampling interval of 2.55 pixels per speckle diameter will avoid both oversampling and undersampling the speckle pattern. In practice, however, it is difficult not to oversample the speckle pattern due to system requirements for the strain measurement resolution, as defined in Equation (4). Generally, the minimum measurable strain occurs for $\Delta A_X = 1$ pixel. Using the Phase II pixel-to-speckle ratio calculation above as an example, it would be necessary to adjust L_0 to be 40.5 mm to give a ratio of 2.55. This would reduce the strain resolution from 15 $\mu\epsilon$ to 370 $\mu\epsilon$ – a significant compromise. In addition, it is impractical to adjust the speckle size by varying the spot diameter on the specimen, because the spot size determines the gage length of the measurement.

Rigid Body Motion Cancellation

The success of this technique in cancelling speckle shift terms due to rigid body motion depends on three factors. First, the geometry of the optical setup must be planar to within some tolerance, which is determined by the maximum values of rigid body motion components it is necessary to cancel. Second, the radius of curvature of the laser beam wavefront L_S at the specimen must be relatively large, again, with the required magnitude depending on the maximum values of rigid body motions encountered. The third requirement is for the speckle patterns to be stationary, to within the resolution of the detector, between exposures from beam 1 and beam 2 during a measurement The first and second requirements are necessary to obtain the simplified speckle-shift relation in Equation (1).

The first requirement can be met by carefully aligning the optics and test specimen, but the second requirement is more of a design consideration. It was shown in previous work[7] that Equation (4) has an error term associated with it in the event of incomplete cancellation of the a_z term:

$$\epsilon_{xx} = \frac{-\Delta A_X}{2L_0 \cdot \sin(\theta)} - \left[\frac{a_z \cdot \cos(\theta)}{L_S}\right] \qquad (22)$$

A value of $L_S \geq 100$ m, for example, would be sufficient to cancel errors due to the out-of-plane translation term a_z, the most sensitive rigid body motion term, for magnitudes of a_z as large as 1.7 mm. Using this value of L_S, decorrelation would actually occur before error is observed. The error term is linear with the ratio a_z/L_S, so given the maximum value of a_z likely to be encountered one can adjust L_S accordingly. Values between 10 and 100 m are typical.

On the practical side, there are different methods of controlling L_S. The standard relationship for the radius of curvature of the laser beam, $L_S(\zeta)$, at a point ζ along its propagation path is given by:

$$L_S(\zeta) = \zeta\left[1 + \left[\frac{b}{2\zeta}\right]^2\right] \qquad (23)$$

where

$$b \equiv \frac{\pi(2\omega_0)^2}{2\lambda} \qquad (24)$$

The variable ζ is the distance from the laser beam waist (the waist is defined as the point of minimum beam diameter, or the transition point between converging and diverging regions of the wave), ω_0 is the waist radius and b is the confocal parameter. The significance of the confocal parameter is that $L_S(\zeta)$ is minimum at $\zeta = b/2$. Parenthetically, the distance b is actually the proper mirror spacing for a confocal resonator.[11] For a setup with the

specimen far away from the beam waist, L_S is equal to the distance from the specimen to the waist; the wave appears to originate from a point source located at the waist. Since the beam waist is typically located near the back mirror of the laser's resonant cavity, large values of L_S would require complicated beam folding. Alternatively, a series of lenses could be used to image the waist far behind the laser, and hence far from the specimen, but this would provide a rather large laser spot on the specimen. This is not desirable because the spatial resolution of the measurement would be decreased.

On the other hand, Equation (23) shows that the wavefront's radius of curvature is infinite at the beam waist and drops off to a minimum of b within a short distance. If the waist were imaged to the plane of the specimen L_S would be quite large. Since the longitudinal region around the waist where the radius of curvature remains large is limited, however, care in positioning the waist would be necessary. This is not a trivial point, because for small beam diameters the confocal parameter is on the order of 1 m and the radius of curvature decreases rapidly away from the waist.

For example, with a waist diameter of 0.6 mm, $L_S(\zeta)$ drops to 6 m a distance 5 cm away. The beam diameter increases by only 2 μm a distance 5 cm away from the waist, making accurate positioning very difficult. The most successful technique for positioning the waist has been to move it through the specimen plane in steps, measuring error cancellation at each step. L_S is large enough if no speckle shift is observed when the specimen is translated out-of-plane.

The third requirement for rigid body motion cancellation is really a limit on the test parameters. If relative movement of the patterns occurs between exposures from beam 1 and beam 2, the simultaneity of the measurement by the two beams is lost. This applies to speckle movement due to either strain or rigid body motion. Any rigid body motions that occur between the two exposures are falsely interpreted as strain, and strain occurring between the exposures is only registered by 50% of its true value.

Limits can be specified for the two sources of speckle shift. Referring to Equation (1.a), rigid body motion components due to a_x and Ω_y must not cause speckle shifts A_X between exposures as large as the pixel pitch in the sensor array.

The strain at any point along the wire depends on the instantaneous load and temperature at that point. At high temperatures or within the plastic response region of the specimen these values can change in a relatively short time. At the standard RS–170 video frame rate of 30 frames per second (fps), data can be acquired for a one-dimensional measurement in under 66 milliseconds. This puts a lower limit on the definition of the quasi-static measurement period. It can be generalized that the maximum strain rate ϵ'_{max} in $\mu\epsilon$/s is the resolution of the system in microstrain times the acquisition rate of the strain data. A resolution of 15 $\mu\epsilon$ is assumed. Since two frames are read per one-dimensional strain point,

$$\begin{aligned} \epsilon'_{max} &= \text{resolution} \cdot \left[\frac{\text{frame rate}}{\text{frames/point}}\right] \\ &= 15\ \mu\epsilon \cdot \left[\frac{30\ \text{Hz}}{2}\right] \\ &= 225\ \mu\epsilon/\text{s} \end{aligned} \tag{25}$$

A maximum strain rate of 225 $\mu\epsilon$/s then is necessary to keep the error to within the resolution limit of the system.

A distinction must be made between error due to rigid body motion, and loss of the original signal due to large rigid body motions. The former has been treated, but the latter still requires some discussion. During the course of a stress-strain run, the speckle patterns shift cumulatively over the series of strain measurmements. The shifted patterns are correlated with a stored set of reference patterns; but since the reference patterns are limited in extent, there will occur some magnitude of shift $\mathbf{A}(X,Y)$ for which the reference and shifted patterns no longer overlap. Since this technique inherently makes a differential

strain measurement, it is possible to update the reference patterns occasionally, and sum the incremental shifts to obtain the total strain over the run. The reference patterns can be updated whenever it is determined that the relative amplitude of the correlation peak drops significantly. In this manner it is possible to track speckle pattern shifts of virtually unlimited magnitude.

The question arises, then, of how far the patterns can shift before new reference patterns must be stored. In the Phase I and II systems, in which 1-D sensor arrays were used, the reference patterns were updated after every strain point in order to insure that the patterns were never lost (off-axis shifts could not be recovered). However, in the proposed Phase IV system an area array sensor can allow much larger off-axis shifts to occur without losing the original patterns. If a 512 x 512 pixel array is used, then the off-axis (vertical) shift term A_Y can extend to ±255 video lines before losing the signal. This assumes that the reference filter is taken from the center of the video frame, closest to the xz plane. If full-field reference speckle patterns are stored, a maximum A_Y of ±511 video lines can occur before the signal is lost. For performance considerations, however, it is not preferable to store full-field reference patterns. Along the other shift axis, the magnitude of allowable horizontal shift A_X depends on the correlation filter length (the filter length is the number of picture elements of the reference pattern used in the correlation). Computer simulations using real speckle patterns show that filters 32 pixels in length can still produce accurate correlations. The maximum shift along the horizontal axis would then be ±(512–32)/2, or ±240 pixels, before the reference filters would need to be updated.

To summarize, it is necessary to provide a beam radius of curvature $L_S \sim 50\text{-}100$ m in order to completely cancel errors in the strain measurements. This is best accomplished by imaging the beam waist at the specimen surface. A systematic trial-and-error approach is used for final adjustment of the waist position. Also, speckle patterns should be static during the acquisition of the exposure pair for each strain point. The maximum shift due to both rigid body motion and strain allowable before updating the reference speckle patterns is ±255 lines along the Y axis, and ±240 pixels along the X axis.

Signal Strength

Another parameter which should be considered is the signal strength, or the average intensity of the fully developed speckle pattern. Since the diameter of the wire is very small, the intensity of the speckle pattern at the sensor is decreased. The photometric intensity $I(x,y)$ for a diffuse reflector is a function of φ, the angle between the direction (x,y) and the normal to the surface element dS, as shown by:

$$I(x,y) = \int_S D \cdot \cos\varphi \, dS \qquad (26)$$

where D is given as a constant, assuming an isotropically reflecting (diffuse) surface.[12] The angle φ varies by ±90° over the illuminated curved surface **S** of the wire; the effective reflecting area of the wire is equal to the projection of the surface area in the direction of the sensor. It is apparent from this result that the photometric intensity due to the curved surface is the same as that of an extended flat surface, less the fraction of the incident laser light not intercepted by the wire. The significance of this is that, given some minimum exposure requirement for correlation and a constant incident light intensity, the exposure time for the photodiode array camera must increase by the same fraction as the incident light lost due to the smaller wire cross-section.

Note that although, in this argument, taking D as a constant assumes incoherent light and does not include interference effects, the extension to coherent interference is straightforward by defining $D(x,y\,;\,x,y)$ as a function of source and sensor coordinates.

In the event that the speckle intensity is too low, cylindrical lenses can be placed in the exposure beam to focus the spot entirely onto the wire. Following the

arguments presented above, this would have no effect on the pixel-to-speckle ratio along the shift axis.

Another possible effect of the wire geometry on the speckle shift relations given by Yamaguchi is due to the magnification factor L_0, the sensor-to-specimen distance. A slight variation in L_0 is introduced by the curvature over the gage area. However, this wire curvature has a negligible effect on the speckle shift relations, for two reasons. First, the change in L_0 over the illuminated region is only $6x10^{-3}$ %, for L_0=1 m and a wire diameter of 120 μm. Second, the reaction of the speckle pattern generated by a weakly anisotropic surface projection (anisotropic in that the angle subtended by the mean spacing of the surface roughness decreases with distance from the center of the gage axis) due to deformation of the surface is weighted by the Gaussian power distribution of the incident beam. To first order, the wire surface is flat over the peak power distribution of the beam, further minimizing the effect of curvature.

CORRELATION TECHNIQUES

The speckle-shift optical strain measurement method is potentially very powerful due to its affinity to electronic processing. Optoelectronic detector arrays have sufficient resolution to record the spatial frequencies found in typical objective speckle patterns. This allows the speckle patterns to be stored and manipulated digitally, providing great flexibility in processing techniques.

The bottleneck in a typical series of strain measurements, however, is presently the time delay introduced by the computationally extensive correlations required to determine the speckle pattern shift vectors. Once each new pair of shifted speckle patterns is recorded, a minimum of two correlations must be performed to calculate the strain. There are various ways that these correlations can be performed, and the goal is to use the technique that is most accurate and dependable, and gives the shortest execution time. Ideally, the processing should be performed within M times the frame period of the image acquisition system, where M is the number of shifted speckle patterns needed for the measurement (M=2 for a 1-D strain measurement). This ideal processing requirement would then place the ultimate speed constraint on the data transfer electronics.

The state-of-the-art in digital signal processors (DSPs) is progressing to the point that they can provide concurrent processing performance heretofore never achieved. Even with mainframe processing power, calculations cannot be done in real-time due to data transfer delays as well as other delays inherent to multi-user systems. The power in DSPs lies in that they are dedicated on-line processing chips, designed with built-in floating point capabilities, performing narrow, programmable, processing functions without the overhead associated with the host computer's CPU.

Three correlation techniques were under consideration for the high speed system; each technique has certain advantages, which are compared below. The three techniques are termed: "spatial" correlation, "spectral" correlation, and "image summing" correlation.

Spatial Correlation

The spatial correlation is a straightforward digital implementation of Equation (5) over shift index range x_{max}:

$$R_j = \frac{1}{N} \sum_{i=1}^{N} f_i \cdot g_{i+j} \qquad (27)$$

where $j = 0,\pm1,\pm2,...\pm x_{max}$ and N is the filter length. The visibility of the correlation peak is improved by subtracting the mean values of f and g before implementing Equation (27). The advantages of this calculation are that it is very accurate, flexible, and fast when using short record lengths. It is possible to directly decrease the number of operations by limiting the correlation range x_{max} to the maximum shift expected during the measurements.

One limitation on the minimum proces-

sing time possible for the speckle correlations is determined by the minimum necessary record length N of each speckle pattern. It must be assured that the speckle patterns are considered wide–sense stationary and ergodic random processes when performing the correlations.[13] The speckle pattern slice used in the cross-correlation should be large enough to satisfy these requirements (this is an issue separate from the pixel-to-speckle ratio). In previous testing, record lengths of 512 and 768 pixels were used with good results.

Spectral Correlation

The spectral correlation, so named because the correlation is performed in spatial frequency space, utilizes the Fourier transform. This technique is based on the cross-correlation version of the Wiener-Khinchin theorem. The reference speckle pattern f(x) and the shifted speckle pattern g(x) are Fourier transformable, so that $\mathcal{F}\{f(x)\} = F(u)$ and $\mathcal{F}\{g(x)\} = G(u)$, where $\mathcal{F}$ denotes the Fourier transform operator. The cross-correlation $R(\Delta x)$ of f and g is given by:

$$R(\Delta x) = f(x) \circledast g(x)$$

$$= \mathcal{F}^{-1}\left\{F^*(u) \cdot G(u)\right\} \qquad (28)$$

where $\circledast$ denotes the correlation operator. The Fourier transforms of the reference and shifted patterns are multiplied together, and the inverse transform $\mathcal{F}^{-1}$ gives the correlation function.[14] This calculation can be performed using an efficient fast Fourier transform (FFT) algorithm. An inherent advantage of this technique is that the correlation is calculated over the entire range of the data array. Therefore, there is no performance penalty for correlating large speckle shifts. In addition, DSPs are well suited for calculating FFTs. One slight performance degradation is the necessity of windowing the data to minimize aliasing artifacts due to artificial high spatial frequencies.

Image Summing Correlation

The third technique mentioned above calculates the auto-correlation of the sum of two speckle patterns. The process is similar to an electronic implementation of double exposure speckle interferometry.[15] The shifted speckle pattern is added point by point to the reference pattern. This summed image is, in essence, a field of speckle pairs offset by a constant shift value. These speckle pairs constitute a dominant spatial frequency in the image. The magnitude of the Fourier transform of these correlated speckle pairs produces Young's fringes; the spacing of these fringes are then inversely proportional to the speckle shift. The final step is to extract the shift between the speckle patterns: The inverse transform of the Young's fringes gives the period of the fringes, from which the speckle pattern shift is calculated.

An advantage of this technique is that it requires only two FFTs per correlation. However, a problem is that, for small shifts, the correlation peak representing the shift is lost in the auto-correlation peak located at the origin. A way around this is to artificially shift the patterns by an amount which is later subtracted from the total shift in the correlation peak; this moves the region of interest away from the origin, where it will not be obscured.

A more important problem with this technique is a directional ambiguity in the shift. The initial addition of the speckle patterns creates a field of speckle pairs, with equal separation, or shift, between the speckles in each pair. When the image is correlated, this spatial frequency is adequately represented by a pair of correlation peaks centered about the origin. But since a reference point is never encoded in the combined image, only the magnitude of the shift is retrievable.

When these three techniques are compared it becomes clear that the spatial correlation technique provides the best response. Since the premise of the high speed system is that the speckle patterns will be updated many times a second, the shifts will be small. The shift index j will not range beyond roughly ±10, giving this

technique a speed advantage over a full range spectral correlation.

ROOM TEMPERATURE TESTS

Until this point, the effects of a change in specimen geometry has been largely in regard to the integrity of the speckle-shift equations. From an experimental viewpoint, when using a specimen of small thermal mass it is important not to induce local heating by the laser beam. This heating causes thermal strain at the gage location which contributes to speckle shifts. Since the shifts are due to real strain, they cannot be cancelled; they will degrade any stress-strain relationship being measured. It is, of course, *not* desirable that the instrument affect the measurement in any way.

During the room temperature tests for this study, thermal strain was observed to be a problem at high power levels. Once the laser output power was reduced from 2 W to 0.5 W, the stability of the speckle patterns over successive exposures increased. For an incident power of 0.5 W and a 30 ms exposure time, the speckle patterns varied between a shift of zero and one diode (which translates to a shift of 0 to 15 μm at a distance of 1 m from the specimen) over a series of twenty exposures (about 20 minutes duration). The correlation function was sharply peaked over the duration of the test. Tungsten and stainless steel wires with diameters of 76 and 813 μm (3 and 32 mils), respectively, were used for these tests.

HIGH TEMPERATURE TESTS

One of the critical questions associated with high temperature optical measurements is whether thermal density gradients during a test are severe enough to prohibit accurate readings. Past testing has indicated problems of this sort at temperatures as low as 450°C. Free convection set up by air temperature/density variations around a hot specimen can result in an unstable phase propagation medium for the speckle-forming laser light. Since a stable speckle pattern depends explicitly on stable phase relationships, dynamic density variations can severely degrade the measurements.

If the density variations occur within a spatial extent smaller than a cross-section of the solid angle subtended between the laser spot and the speckle pattern on the sensor, the speckle pattern will exhibit a boiling action. If, on the other hand, the phase medium varies on a scale larger than the cross-section of this solid angle the speckle pattern will jitter or vibrate as a field. The latter case was observed during Phase I testing. In Phase II the specimen was enclosed in a thermally insulating box. Subsequently, the jitter effect was not observed at test temperatures beyond 750°C.

Thermal effects of the first kind cannot be compensated for if they exceed some minimum necessary to maintain correlation between exposures. However, the situation is different for speckle shifts due to thermal variations of the second kind, those on a scale larger than the aforementioned solid angle. These shifts can be cancelled as rigid body motions if the shifted speckle pattern pair can be acquired fast enough to stop the relative movement of the thermal zone between exposures.

Further experiments were necessary to determine if the problem would recur at the much higher temperatures desired for future materials testing. An ac light bulb was used to provide a hot wire specimen. The bulb provided a means of testing a tungsten alloy in an inert atmosphere using standard hardware. The glass envelope sealed the wire filament in dry nitrogen gas to prevent oxidation of the tungsten. The operating pressure in the envelope was estimated to be ≈1.5 atm. The envelope was transparent and cylindrical in shape (measuring 9 by 3 cm), allowing the necessary optical access for the laser beams and speckle patterns. A variac was used to adjust the voltage across the filament without clipping the ac signal, effectively varying the filament temperature. A calibration of temperature versus line voltage was obtained from the bulb manufacturer.

The filament was made from a 37 μm (1.5 mil) diameter wire of W–Re alloy.

The wire was tightly wound into a 122 μm (4.8 mil) diameter filament. It has been observed in high temperature testing that speckle pattern movements can stem from three sources:

1) Strain along the sensitive axis of the gage;
2) Rigid body motions of the specimen, including rotations and translations, caused by either mechanical or thermal sources (a change in temperature anywhere along the specimen can translate the test section through thermal strain);
3) Instabilities of the phase propagation medium between the specimen and sensor.

Using the bulb's filament as a specimen had the fortuitous advantage of separating speckle movement source 3) from sources 1) and 2). The coiled filament absorbed the thermal strains in the coils, which tended to inhibit translations of the bulk filament. This made it possible to isolate the test from all effects except those of the propagation medium. The speckle statistics accurately obeyed those of a 122 μm diameter solid wire. A series of speckle patterns were recorded and correlated with a single pair of reference patterns at a specimen temperature of 2,480°C. Excellent stability was observed in the high temperature tests, indicating that the isolation provided by the glass envelope was sufficient to avoid thermally induced jitter. The correlation peak occurred at shift values of 0 and 1 pixels over time, which is within the resolution of the correlation algorithm. Figures 3.a and 3.b show a set of reference and shifted speckle patterns, and their correlation over a shift range of ±60 pixels. Since the wire was subjected to neither load nor rigid body motion, there should be no offset between the patterns. Indeed, the correlation in Figure 3.b is sharply peaked at an offset of zero, as expected. The speckle pattern stability was also very good at room temperature and 1,825°C.

It is important to note that these results alone do not guarantee accurate measurements at high temperatures using a straight wire specimen. Acquisition of the speckle pattern pairs must always occur fast enough to stop the action of any translations of the specimen or changes in the strain state at the gage position. A detailed discussion is given in the Advanced System Requirements section.

Background Radiation

Background radiation levels at these high temperatures are significant within the sensitive band of the detector array. A line pass interference filter, tuned to the laser output wavelength of 514.5 nm, has been used to attenuate blackbody radiation from the specimen. Since this thermal radiation comes from an extended source and no imaging system is used, the background light is roughly dc. The filter is simply used to increase the dynamic range of the speckle signal by attenuating the dc signal.

There could exist, however, some test situations in which background radiation at the laser wavelength becomes intense enough to dominate the speckle data, even when using a line pass filter. Not only is the temperature of the specimen a factor in this situation, but the solid angle Ω_s of the blackbody source also factors directly into the exposure of the detector. Specimens may be heated in clamshell style heaters whose internal walls are essentially the same temperature as the specimen. The detector array would look at the specimen through a quartz port which simulates a blackbody emitter. At some temperature, the blackbody radiation emitted from the port would reach a level that saturates the array, regardless of the speckle exposure level. Using this saturation as an indicator, a maximum test temperature can be estimated.

The spectral radiance at wavelength λ and temperature T is given by Planck's distribution law:

$$i_\lambda(T) = \frac{2hc^2}{\lambda^5 \cdot \left[e^{\left[\frac{hc}{\lambda kT}\right]} - 1 \right]} \qquad (29)$$

in $W/(m^2 \cdot m \cdot sr)$, where h is Planck's constant and k is Boltzmann's constant.[16] The speed of light c in vacuum can be divided by the refractive index of the medium. For this calculation, however, Equation (29) is a good approximation (the refractive index of a gas is nearly unity). Assuming the port to be an ideal blackbody source, the emissivity is also taken as unity. Referring to Figure 2, the spectral irradiance I at the detector for a given wavelength is

$$I = i_\lambda(T) \cdot \Omega_d \left[\frac{A_s}{A_d}\right]$$

$$= i_\lambda(T) \cdot \left[\frac{A_d}{r^2}\right] \cdot \left[\frac{A_s}{A_d}\right]$$

or, $$I = i_\lambda(T) \cdot \Omega_s \qquad (30)$$

where Ω_d and Ω_s are the solid angles subtended by the detector and the source, respectively, A_d and A_s are the areas of the detector and the source, respectively, and r is the distance between the detector and the source. The line pass filter in front of the detector has a bandwidth of 9 nm centered at 514.5 nm, which makes it necessary to integrate Equation (30) over this wavelength interval in order to find the power on the detector from the thermal source.

A simpler and equivalent procedure is to calculate the total irradiance from the source, and multiply by the fraction of the irradiance in the wavelength band from λ_1 to λ_2. The total radiance i is calculated by integrating Equation (29) over all wavelengths, giving the standard equation

$$i = \frac{\sigma T^4}{\pi} \qquad (31)$$

where the Stefan-Boltzmann constant

$$\sigma = \frac{2(\pi k)^4}{15h^3c^2} \left[\frac{W}{m^2 \cdot K^4}\right] \qquad (32)$$

The fraction of i is given by:

$$F_{\lambda_1 \to \lambda_2} = \frac{\int_{\lambda_1}^{\lambda_2} i_\lambda \, d\lambda}{\int_0^\infty i_\lambda \, d\lambda}$$

$$= \frac{\pi}{\sigma T^4} \int_{\lambda_1}^{\lambda_2} i_\lambda \, d\lambda \qquad (33)$$

or equivalently,

$$F_{\lambda_1 \to \lambda_2} = \frac{\pi}{\sigma T^4} \left[\int_0^{\lambda_2} i_\lambda \, d\lambda - \int_0^{\lambda_1} i_\lambda \, d\lambda \right] \qquad (34)$$

This can be rearranged into a more universal form using the parameter λT:

$$F_{\lambda_1 \to \lambda_2} = F_{\lambda_1 T \to \lambda_2 T} \qquad (35)$$

where

$$F_{\lambda_1 T \to \lambda_2 T} = \frac{\pi}{\sigma} \left[\int_0^{\lambda_2 T} \frac{i_\lambda}{T^5} \, d(\lambda T) - \int_0^{\lambda_1 T} \frac{i_\lambda}{T^5} \, d(\lambda T) \right] \qquad (36)$$

$$= F_{0 \to \lambda_2 T} - F_{0 \to \lambda_1 T} \qquad (37)$$

The irradiance then becomes

$$I = i_{\lambda_1 \to \lambda_2}(T) \cdot \Omega_s \ (W \cdot m^{-2}) \qquad (38)$$

$$= \left[\frac{\sigma T^4}{\pi}\right] \cdot \left[F_{0 \to \lambda_2 T} - F_{0 \to \lambda_1 T}\right] \Omega_s \qquad (39)$$

The fractions in Equation (39) are available in blackbody tables for various values of λT. By choosing a number of temperatures, the irradiance of Equation (39) can match the saturation irradiance of the detector. The temperature at which this occurs is then an estimate of the maximum temperature at which the speckle-shift strain measurement system will operate.

A reasonable saturation exposure for a charge coupled device is 0.03 $J \cdot m^{-2}$, requiring the irradiance necessary to saturate the array over the integration time to be about 2 $W \cdot m^{-2}$. If the detector is 0.95 m away from a port 1 cm in diameter, $\Omega_s = 9 \times 10^{-5}$ sr, the filtered irradiance given by Equation (39) then exceeds the saturation irradiance of the array at temperatures around 3,300°C.

Specimen Type and Survivability

Wire specimens, of the type used in high temperature composite materials, were chosen for the Advanced System application. Wires (or fibers) are ideal specimens for the one-dimensional strain measurement system because their loading in a material or a structure is generally longitudinal by design. The 1-D system excels at measuring longitudinal strain. The best temporal response of the two-beam speckle-shift technique is achieved when making a one-dimensional measurement, because the speckle data for this measurement can be acquired in the least time. A two-dimensional measurement requires either a mechanical rotation of the optical system, which can destroy the simultaneity of the measurement, or a complicated beam switching system that would not only make alignment much more difficult, but greatly increases the data acquisition time.

Tungsten is an element slated for use in high temperature materials due to its strength and high melting point. It unfortunately has a strong affinity to oxidation, and must, therefore, be protected from oxygen at high temperatures. This may be done in composites by sheathing or sealing the reinforcing tungsten wires in a matrix impervious to oxygen. Such a seal is difficult to maintain under loading, however and has caused problems of long term survivability. In the testing done here the specimen was surrounded by a gaseous N_2 atmosphere at high temperatures.

Room temperature tests on straight tungsten wires were successfully conducted in the open air. Some specimens were gradually heated resistively, but in this open air environment it was not possible to take measurements at any appreciable temperatures – the specimens burned too quickly.

However, other materials, such as ceramics, are well suited to an oxidizing environment. Alumina (Al_2O_3) is extremely stable at high temperatures, although it makes a relatively weak fiber. Carbon fibers can also tolerate the high temperatures of interest here. Silicon carbide (SiC) is another good reinforcing fiber.

An important consideration when using ceramic specimens, however, is their reflective property for electromagnetic radiation. Ceramics tend to have multiple-reflecting surfaces, due to their electronic band structure, which prevent generation of a fully developed speckle pattern. Such depth in a surface destroys the coherent property of the laser light, reducing the visibility, or contrast, of the signal. This also brings on the possibility that bulk anisotropies in the material would decorrelate the speckle patterns. Future choices of test specimens should address these issues.

ADVANCED SYSTEM REQUIREMENTS

The Advanced System effort will concentrate on developing a one-dimensional measurement system capable of calculating

strains using a high speed processor. It will provide the ability to continuously track off-axis speckle movements. By updating the reference speckle patterns when off-axis movements occur, decorrelation effects will diminish and the measurement range of the instrument will increase. In addition, the alignment criteria for the specimen will not be as stringent, and a less specialized load machine will be required.

In past speckle-shift systems a linear photodiode array has been used to record a 1-D slice of the extended speckle pattern with high spatial resolution. As mentioned in the section on the speckle-shift technique, ideal conditions minimize off-axis speckle shifts A_Y. However, certain rotations and translations of the specimen during loading can cause this reference slice to shift off the one-dimensional array, making further correlations impossible. This makes careful alignment of the load machine and specimen, as well as the instrument optics, critical to the success of the measurement; these rigid body motion terms can be suppressed with enough care. Unfortunately, standard test rigs often do not have the precise positioning capability needed to suppress the critical specimen movements during a run.

Recent developments in state-of-the-art area sensor arrays have increased their resolution and reliability to the point that a full field speckle pattern can now be easily recorded electronically by the system. The reference correlation filter shifted by vector $A(X,Y)$ on a 2-D array is represented by the shaded rectangle in Figure 1. When the speckle patterns shift off-axis during a run, the reference slice will still be on the two-dimensional sensor array and correlation will be maintained. On the other hand, the processing speed will need to increase to meet the demands of this improvement. It will be necessary to perform a number of correlations per strain point to track the speckle shifts. The reference patterns must be correlated with lines on the array both above and below the reference coordinate. This is essentially a two-dimensional correlation of limited extent. To minimize the processing time the shift index j in Equation (27) will vary about the previous peak location in the X direction. Similarly, the off-axis line search will begin with the previous off-axis shift value.

The optical system required for the Advanced System is very similar to the Phase II optical system. The only change is in the omission of two items – the goniometer, which was used to acquire different strain components on the specimen, and the $\lambda/4$ retardation plates, which were necessary when using the goniometer.

Concurrent Processing

Concurrent processing of the speckle data simply means that the speckle shifts are determined and the strain calculated before collecting more data. In the ideal case, the calculations are performed as fast as the data can be collected.

To determine the required calculation time between strain points one must know how many image lines need to be correlated before the maximum correlation peak is found. If the correlation peak is found within two or three lines, then the measurement can proceed sooner than if, say, twenty lines must be correlated before finding the maximum peak. A situation of increasing returns also enters into the situation: the faster the correlations can be computed the fewer lines need to be correlated, simply because the specimen has less time to move between frames.

By assuming that off-axis shifts occur at a rate no greater than shifts due to strain, the maximum strain rate given above dictates a maximum off-axis shift of one pixel per frame. A high resolution camera has a pixel spacing of 6.8 μm. Because either positive or negative shifts can occur, and including a safety factor of two, the measurement requires four lines to be correlated per beam per strain point. Therefore, use of *two* beams requires eight correlations to be calculated within 66 ms. The minimum performance criterion, then, is roughly 8 ms per correlation, including data transfer time and system overhead. This calculation time is within the margin of available state-of-the-art performance, however, actual testing will determine if

the data transfer times and system overhead is sufficiently low.

Post-Processing

An alternative to the concurrent processing technique is post-processing. If full field speckle patterns can be stored at the desired frame rate (the frame rate may even be faster than the standard 30 fps) for the duration of the run, the processor can perform the correlations at a non-critical rate after the data are acquired. The limits on the run, e.g strain rate and duration, then rest on the storage speed and capacity of the data acquisition system. Since the processing time between points is not a limiting factor, data at very high strain rates can be acquired in the presence of very large rigid body motions.

When using a 512 by 512 element array, the system requires 1/4 Mbytes of storage per frame and 1/2 Mbytes per strain point. With a period of 33 ms per frame, a data transfer/storage rate of at least 8 Mbytes/sec is necessary. Image storage systems with this performance are available on the market. Images up to 1024 by 1024 pixels in size can be stored at RS–170 frame rates on an array of hard disks, with storage capacities in the Giga-byte range.

A drawback of post-processing is that neither the operator nor the control system has strain information available during the run. This is acceptable if the test requires, say, a constant pulling rate until specimen failure occurs, but not if it is necessary to apply a constant strain rate to the specimen.

CONCLUSIONS

The high temperature behavior of speckle patterns has been studied using small diameter wire specimens. Stable speckle patterns have been observed over extended periods of time at temperatures up to 2,480° Celsius. Accurate correlations were performed. No degradation due to refractive index changes has been observed when the hot wires are enclosed in a glass envelope.

The speckle-shift relations remain valid for measuring longitudinal strain on small diameter specimens. Speckle statistics along the longitudinal axis are uncorrelated to those of the transverse axis.

Use of the repeated one-dimensional "spatial" correlation as the peak tracking method will provide optimal performance for the limited shifts encountered using the speckle-shift technique. Defining a reasonable filter size can provide better performance than FFT based correlation techniques. State-of-the-art digital signal processors have the processing speed necessary to calculate cross-correlations at the RS-170 video frame rate. These DSPs are available on standard PC expansion boards. Questions remain whether system overhead reduces the usable frame rate.

The maximum speckle shift that can occur between the two successive camera exposures used to cancel rigid body motion errors is determined by the spatial resolution of the optical system. This basically limits the steady state strain rate to below 225 $\mu\epsilon/s$ when acquiring speckle data at the standard RS-170 frame rate.

It is recommended that future work include use of a two-dimensional CCD array sensor to track off-axis shifts, and development of a concurrent processing system.

REFERENCES

1. Yamaguchi, I.: A Laser-speckle Strain Gauge. J. Phys. E. Sci. Instrum., vol. 14, no. 11, Nov. 1981, pp. 1270-1273.

2. Voorhes, D.; Wyntjes, G.; and Hercher, M.: A Non-contact, Real Time Laser Extensometer for Hostile Environments. Fifth Annual Hostile Environments and High Temperature Measurements Conference, Society for Experimental Mechanics, Bethel, CT, 1988, pp. 53-58.

3. Wu, T.T.; Ma, L.C.; and Zhao, L.B.: Development of Temperature-compensated Resistance Strain Gages for Use to 700°C. Exper. Mech., vol. 21, no. 3, Mar. 1981, pp. 117-123.

4. Wu, T.T.; and Ma, L.C.: Comparison of Characteristics of Our Temperature-compensated Resistance Strain Gages for Use to 700°C and 800°C. Fourth Annual Hostile Environments and High Temperature Measurements Conference, Society for Experimental Mechanics, Bethel, CT, 1987, pp. 30-34.

5. Grant, H.P.; Anderson, W.L.; and Przybyszewski, J.S.: Rotating Tests of Advanced High Temperature Wire and Thin-film Strain Gages. AIAA Paper 88-3146, July 1988.

6. Hunter, A.R.; and Martinson, R.H.: Strain Measurements at High Temperatures by Optical Methods. Fifth Annual Hostile Environments and High Temperature Measurements Conference, Society for Experimental Mechanics, Bethel, CT, 1988, pp. 68-69.

7. Lant, C.T.; and Qaqish, W.: Optical Strain Measurement System Development – Phase I. Sverdrup Technology, Inc., NASA Contract NAS3-24105, NASA CR-179619, 1987.

8. Lant, C.T.: Two-dimensional High Temperature Optical Strain Measurement System – Phase II. Sverdrup Technology, Inc., NASA Contract NAS3-25266, NASA CR-185116, 1989.

9. Papoulis, A.: Probability, Random Variables, and Stochastic Processes. 2nd ed., McGraw-Hill, 1984, pp. 125-127.

10. Bracewell, R.N.: The Fourier Transform and Its Applications. 2nd ed., McGraw-Hill, 1978, pp. 142-143.

11. Verdeyen, J.T.: Laser Electronics. Prentice-Hall, 1981, pp. 59-60.

12. Born, M.; and Wolf, E.: Principles of Optics. 6th ed., Pergamon Press, 1980, pp. 181-182.

13. Papoulis, A.: Probability, Random Variables, and Stochastic Processes. 2nd. ed., McGraw-Hill, 1984, pp. 219-220, 245-251.

14. Yu, F.T.S.: Optical Information Processing. John Wiley & Sons, 1983, pp. 10-11.

15. Stetson, K.A.: A Review of Speckle Photography and Interferometry. Opt. Eng., vol. 14, no. 5, Sept.-Oct. 1975, pp. 482-489.

16. Siegel, R.; and Howell, J.R.: Thermal Radiation Heat Transfer. 2nd. ed., McGraw-Hill, 1981.

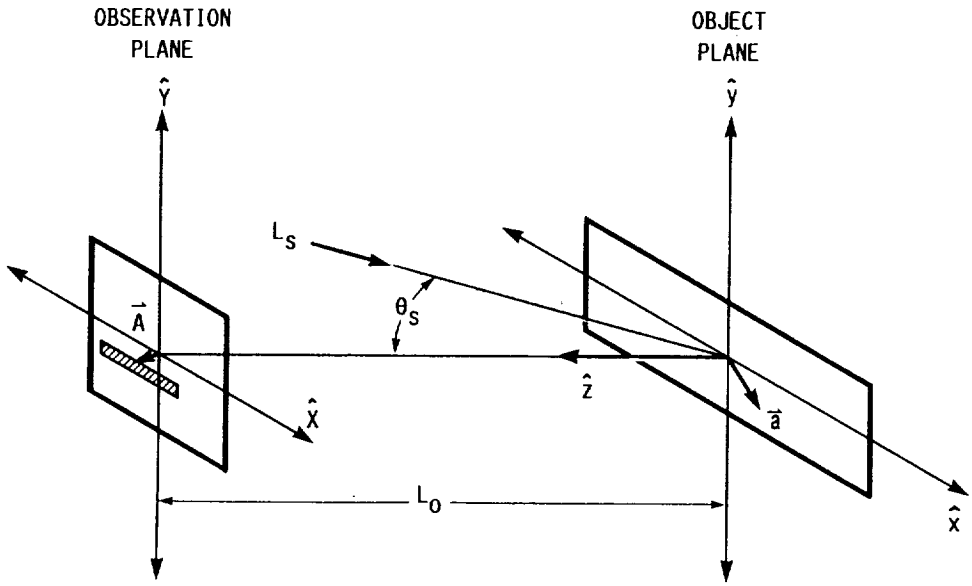

FIGURE 1. - SIMPLIFIED COORDINATE SYSTEM.

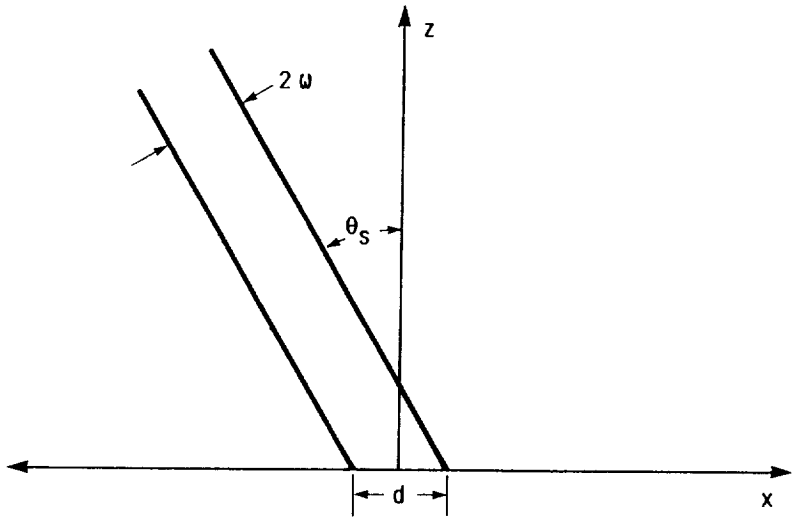

FIGURE 2. - BEAM ELONGATION.

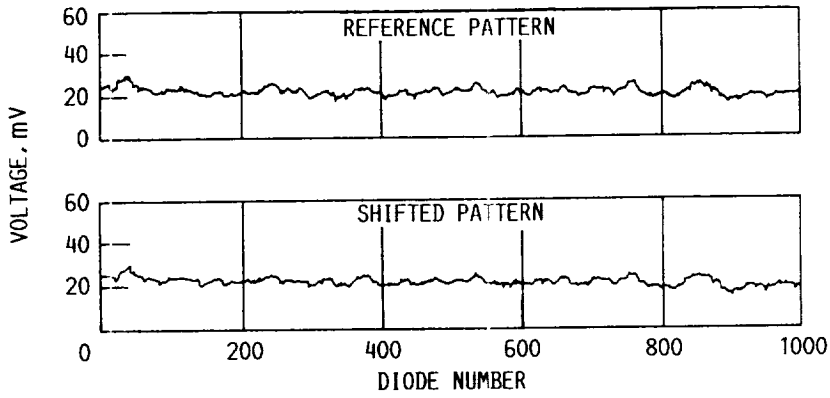

(a) REFERENCE AND SHIFTED SPECKLE PATTERNS.

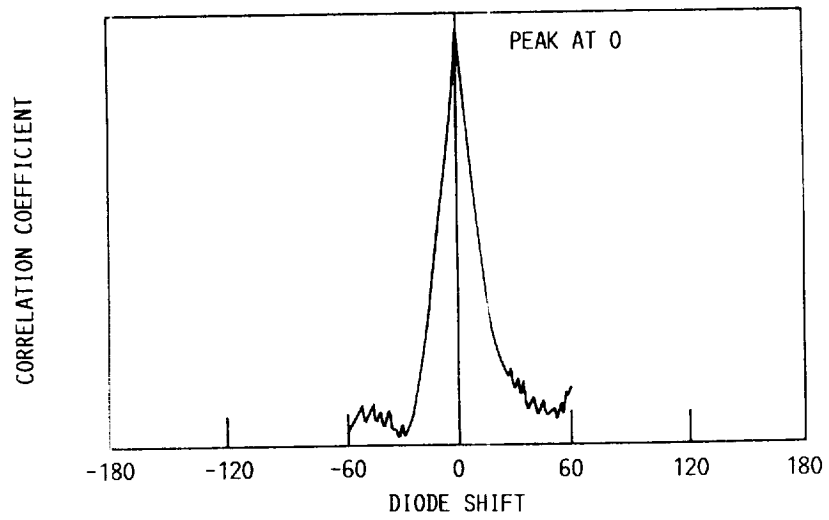

(b) CORRELATION.

FIGURE 3. - TYPICAL SPECKLE PATTERNS AND THEIR CORRELATION, FOR A TUNGSTEN WIRE AT 2480 ^{o}C.

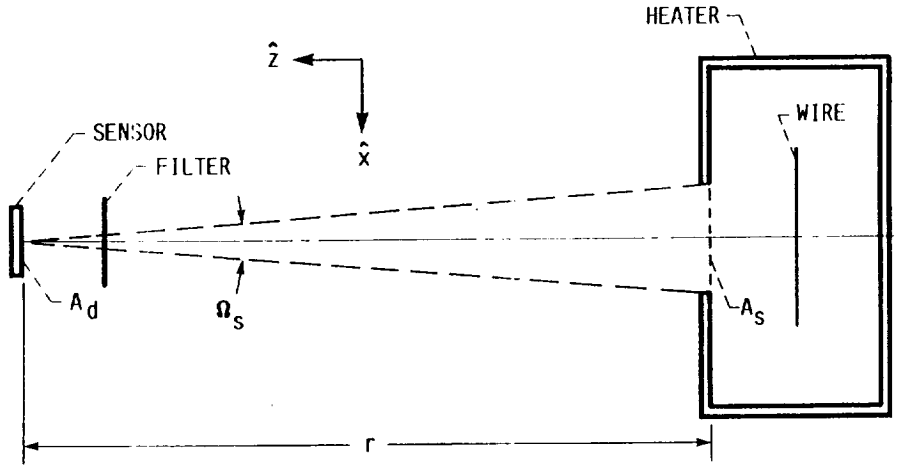

FIGURE 4. - BLACKBODY RADIATION GEOMETRY.

NASA
National Aeronautics and Space Administration

Report Documentation Page

1. Report No.	2. Government Accession No.	3. Recipient's Catalog No.
NASA CR-185254		

4. Title and Subtitle	5. Report Date
Feasibility Study for the Advanced One-Dimensional High Temperature Optical Strain Measurement System – Phase III	6. Performing Organization Code

7. Author(s)	8. Performing Organization Report No.
Christian T. Lant	None (E-5546)
	10. Work Unit No. 582-01-11

9. Performing Organization Name and Address	11. Contract or Grant No.
Sverdrup Technology, Inc. Lewis Research Center Group 2001 Aerospace Parkway Brook Park, Ohio 44142	NAS3-25266
	13. Type of Report and Period Covered Contractor Report Final
12. Sponsoring Agency Name and Address	14. Sponsoring Agency Code
National Aeronautics and Space Administration Lewis Research Center Cleveland, Ohio 44135-3191	

15. Supplementary Notes

Project Manager, John P. Barranger, Instrumentation and Control Technology Division, NASA Lewis Research Center.

16. Abstract

The Instrumentation and Control Technology Division is developing optical strain measurement systems for applications using high temperature wire and fiber specimens. This feasibility study has determined that stable optical signals can be obtained from specimens at temperatures beyond 2,400 °C. A system using an area array sensor is proposed to alleviate off-axis decorrelation arising from rigid body motions. A digital signal processor (DSP) is recommended to perform speckle correlations at a rate near the data acquisition rate. Design parameters are discussed, and fundamental limits on the speckle shift strain measurement technique are defined.

17. Key Words (Suggested by Author(s))	18. Distribution Statement
Laser speckle; Correlation; High temperature strain measurement; Optical measurement; Diffraction; Spatial frequency; Sampling	Unclassified – Unlimited Subject Category 35

19. Security Classif. (of this report)	20. Security Classif. (of this page)	21. No. of pages	22. Price*
Unclassified	Unclassified	20	A03

NASA FORM 1626 OCT 86

*For sale by the National Technical Information Service, Springfield, Virginia 22161